Drug Delivery and Translational Research
https://doi.org/10.1007/s13346-019-00681-8

ORIGINAL ARTICLE

Biodegradable and biocompatible spherical dendrimer nanoparticles with a gallic acid shell and a double-acting strong antioxidant activity as potential device to fight diseases from "oxidative stress"

Silvana Alfei[1] · Silvia Catena[1] · Federica Turrini[1]

Abstract

Gallic acid (GA) is a natural polyphenol with remarkable antioxidant power present in several vegetables and fruits. A normal feeding regime leads to a daily intake of GA which is reasonably regarded as "natural" and "safe" for humans. It owns strong potentials as alternative to traditional drugs to treat several diseases triggered by oxidative stress (OS), but poor gastrointestinal absorbability, pharmacokinetic drawbacks, and fast metabolism limit its clinical application. In this work, a fifth-generation polyester-based dendrimer was firstly prepared as a better absorbable carrier to protect and deliver GA. Then, by its peripheral esterification with GA units, a GA-enriched delivering system (GAD) with remarkable antioxidant power and high potential against diseases from OS was achieved. Scanning electron microscopy results and dynamic light scattering analysis revealed particles with an average size around 387 and 375 nm, respectively, and an extraordinarily spherical morphology. These properties, by determining a large particles surface area, typically favour higher systemic residence time and bio-efficiency. Z-potential of − 25 mV suggests satisfactory stability in solution with tendency to form megamers and low polydispersity index. GAD showed intrinsic antioxidant power, higher than GA by 4 times and like prodrugs, and it can carry contemporary several bioactive GA units versus cells. In physiological condition, the action of pig liver esterase (PLE), selected as a model of cells esterase, hydrolyses GAD to non-cytotoxic small molecules, thus setting free the bioactive GA units, for further antioxidant effects. Cytotoxicity studies performed on two cell lines demonstrated a high cell viability.

Keywords Gallic acid · Biocompatible dendrimer particles · Gallic acid delivery device · Radical scavenging activity · Pig liver esterase · Spherical nanoparticles

Introduction

Oxidative stress (OS) is caused by the accumulation of free oxygen and nitrogen radical species (ROS and RNS) in the cells and is considered the key triggering factor for several human disorders, including cardiovascular malfunction, cataracts, cancer, rheumatism, and many other auto-immune and neurodegenerative diseases and ageing [1].

A number of synthetic drugs may provide protection against the deleterious effects of OS, but these are also associated with adverse side effects [1]. Phytochemicals present in unprocessed or minimally processed plant foods, in addition to the basic nutritional value, own extra health benefits and can be considered "pharmaceutical-grade nutrients".

In particular, polyphenols, such as hydroxyl benzoic acids (HBAs), form an important class of naturally occurring bioactive entities, having innumerable biological activities, all attributable to their remarkable antioxidant power. HBAs possess the ability to scavenge reactive species such as superoxide radicals and hydroxyl radicals, to reduce lipid peroxyl radicals and to inhibit lipid peroxidation, thus protecting cells from OS via a number of pathways [1, 2]. Among HBAs, gallic acid (3, 4, 5-trihydroxybenzoic acid) **1** (Fig. 1) is a

Silvia Catena and Federica Turrini contributed by determining the RSA% by DPPH test.

Electronic supplementary material The online version of this article (https://doi.org/10.1007/s13346-019-00681-8) contains supplementary material, which is available to authorized users.

✉ Silvana Alfei
alfei@difar.unige.it

[1] Dipartimento di Farmacia, Sezione di Chimica e Tecnologie Farmaceutiche e Alimentari, Università di Genova, Viale Cembrano 4, I-16148 Genova, Italy

Published online: 18 October 2019

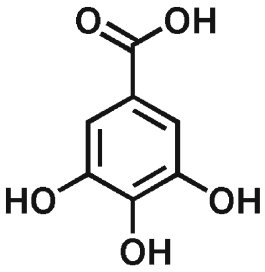

Gallic acid (GA) **1**

Fig. 1 Structure of Gallic acid (GA) **1**

low molecular weight, tri-phenolic acid, extensively distributed in many different families of plants, and contained in common foodstuffs.

It can be found both in the free state and as a part of more complex molecules, i.e. as aglycone, bound to its food matrix, as ester derivatives or in polymeric forms known as gallotannins (GTs). After food consumption or its oral administration as pure compound, GA is slowly absorbed in gastrointestinal tract (GIT) and, after fast metabolism, it is excreted in the urine as 4-*O*-methylgallic acid. Its ester derivatives, such as catechin gallate esters and GTs, are firstly hydrolysed to GA and then metabolised to methylated derivatives [3]. GA is an efficient apoptosis inducing agent that, thanks to a fine amalgam between its antioxidant and pro-oxidant power, fits a large range of applications both clinical, and industrial. GA is able to exert strong antioxidant activity also in emulsion or lipid systems [4, 5] and is used in processed foods, cosmetics, and food packing materials to prevent rancidity induced by lipid peroxidation and food spoilage. GA is also a potent inhibitor of iron and NADPH-dependent microsomal lipid peroxidation but is ineffective against xenobiotic-induced lipids oxidation [6]. It showed neuroprotective actions in different animal models of neurodegeneration, neurotoxicity, and OS as well as anti-mutagenic and anti-carcinogenic activity [7–9].

Unfortunately, the therapeutic application of GA is limited by its pharmacokinetic drawbacks and oral poor bioavailability [10, 11]. Other phenols, such as ferulic acid or *p*-coumaric acid, are adsorbed by the monocarboxylic acid transporter (MCT), whereas GA is not. The serum pharmacokinetic profile obtained from studies in rats showed that GA is slowly absorbed, with a t_{max} for intact GA of 60 min and a max concentration (C_{max}) of 0.71 μmol/L [12], value irrelevant to provide a therapeutically valid antioxidant effect.

Furthermore, GA undergoes a very fast metabolism that translates in an insignificant drug-life. Its major metabolites, i.e. 4-*O*-methylgallic acid and pyrogallol, are in turn promptly metabolised to other molecules that, both possess less antioxidant activity and are speedily excreted in the urine [13].

In order to not waste the GA strong potentialities for human's wellness, researcher efforts are increasingly focused on implementing strategies to overcome GA pharmacokinetics limitations [10, 14, 15].

Nanoparticles [16–19] are widely investigated to prepare multifunctional platforms [20] and are extensively adopted in several biomedical applications [21–29]. Among nanoparticles, dendrimers are highly branched and symmetric macromolecules, characterised by a monodisperse tree-like structure, with both internal cavities for guest molecule entrapment and many peripheral groups that allow further functionalisation. Differently from traditional polymers, they have an unusually low intrinsic viscosity that consents their easy transport in the blood [30, 31] and are characterised by a very low PDI < 1.1 or are even monodispersed [32]. These nonpareil properties make dendrimers ideal carriers both for gene and drug delivery (DD). In DD, they allow to control molecular weight, hydrophilicity, solubility [33–35], bioavailability, and pharmacokinetic behaviour of transported drugs.

Dendrimers offer the possibility to anchor active directing agents, allowing cell-targeted therapies [36–38]. Dendrimers are also capable of establishing strong interactions with several drugs, thus facilitating drug loading and limiting systemic toxicity by minimising the initial massive drug release in parenteral administration [33–35].

Well-known poly(amidoamine) dendrimers (PAMAMs) have been and are unceasingly under study both for drug and gene delivery applications [39, 40]. Unfortunately, due to their amine-terminated, not biodegradable scaffold and to the excessive positive charge, spread across the whole surface, PAMAMs frequently interact, non-specifically with negative charges of biological membranes. As direct consequence, several problems occur, such as cytotoxicity, haemolytic toxicity, and fast clearance from the blood circulation, as well as high level of uptake in the reticuloendothelial system. For these reasons PAMAMs, if not properly modified, are not advisable for clinical applications [41]. Uncharged dendrimer matrices, decorated with protonable amino acid residues [42–45], represent a better and less toxic alternative [46–49]. Within this category, polyester dendrimer scaffolds are the most attractive, because of their good biodegradability [32, 50, 51].

Against this background, the first scope of this work was to develop a successful strategy, resorting to dendrimer nanoparticles, for ameliorating GA Lipophilic Hydrophilic Balance (LHB) and gastrointestinal absorbability, for limiting its pharmacokinetic drawbacks and for opposing its fast metabolism and pro-oxidant counterpart. In this regard, a fifth-generation polyester-based dendrimer, built on the di-functional *core* 1, 3-propandiol (**4**) was prepared. The so obtained dendrimer **4,** thanks to its sixty-four OH peripheral groups (**4**) exploitable for binding GA, was used as a permeability enhancer carrier [52] for promoting a more efficient GA administration. Therefore, **4** was peripherally esterified with bioactive GA

units, achieving a biodegradable GA-dendrimer prodrug (GAD) **9**, endowed with high molecular weight (MW), uncommon particles size of about 380 nm, particles morphology amazingly spherical and consequently large surface area, that typically increase the drug delivery systems (DDSs) systemic retention time, favouring higher bio-efficiency [52]. The second scope of the present study was, to perform significant "preliminary tests", to assess whether GAD could have any potentiality to be subsequently taken into consideration for more in-depth and specific evaluations concerning its actual activity against disorders triggered by OS. In this regard, GAD was firstly investigated to evaluate its antioxidant power, a key and mandatory property to be able to hope for possible therapeutic properties against diseases caused by OS. Then, additional investigations, to evaluate its behaviour in an *in vitro* simulation of the physiological conditions inside the cell, where esterase hydrolytic attacks may occur, were also performed, with exciting results. Finally, cytotoxicity studies on two opportunely selected cell lines were performed to exclude any damage to the cells by exposure to GAD.

Materials and methods

Materials and Instruments

All the reagents including pig liver esterase (carboxylic-ester hydrolase) and solvents were purchased from Merck (e.g. Sigma-Aldrich). Reagents were used without further purifications, while solvents were dried and purified by distillation according to standard procedures. Petroleum ether refers to the fraction with boiling point 40–60 °C. Dendrons D4BnA, D4BnOH, D5BnA, and **2** were prepared as previously reported [53–55]. Melting points were determined on Mettler Toledo MP50 Melting Point System and are uncorrected. FT-IR spectra were recorded as films or KBr pellets on a Perkin Elmer System 2000 spectrophotometer. ^{1}H and ^{13}C NMR spectra were acquired on a Bruker Avance DPX 300 Spectrometer at 300 and 75.5 MHz, respectively, and assigned through DEPT-135 and decoupling experiments. Coupling constant values were given in Hertz. Fully decoupled ^{13}C NMR spectra were reported. Chemical shifts were reported in δ (parts per million) units relative to the internal standard tetramethylsilane (δ = 0.00 ppm) and the splitting patterns were described as follows: s (singlet), d (doublet), t (triplet), q (quartet), m (multiplet) and br (broad signal). Centrifugations were performed on an ALC 4236-V1D Centrifuge at 3400–3500 rpm. Freeze-drying was performed on an EDWARDS Super Modulyo Freeze Dryer, Ice capacity 8 kg, 8 kg/24 h, refrigeration down to − 55 °C with 24-place Drum Manifold. Dynamic light scattering (DLS) was performed on a Malvern Zetasizer Nano ZS instrument (Southborough, MA). Gas chromatography analysis was carried out using a Varian 3400 gas chromatograph connected to a Finnigan MAT SSQ710A mass spectrometer. Chromatographic separation was performed with a RTX-5MS (Restek Corporation) capillary column (30 m × 0.25 mm i.d., 0.25-μm film thickness). Scanning electron microscopy (SEM) images were obtained with a Leo Stereoscan 440 instrument (LEO Electron Microscopy Ltd). Thin layer chromatography (TLC) system employed aluminium-backed silica gel plates (Merck DC-Alufolien Kieselgel 60 F254) and detection of spots was made by UV light. Elemental analyses were determined by an EA1110 Elemental Analyser (Fison Instruments). Organic solutions were dried over anhydrous magnesium sulphate and were evaporated using a rotatory evaporator operating at reduced pressure of about 10–20 mmHg.

Synthesis of compounds 3-9

Compounds **3**-**9** were prepared according to the synthetic paths described in Schemes 1 and 2. Experimental details were reported in Table S1 in Electronic Supplementary Material (ESM) (Section S1). Synthetic and purification procedures are available in Sections S1-S3 in ESM. An additional table (Table 1), reporting the yield (%) of all the intermediates, except for not isolated compound **8**, and of final product GA-dendrimer (**9**), is available in the "Results and discussion" section.

Physicochemical characterisation of compounds 3-9

Spectroscopic and Elemental analysis data

FT-IR, NMR, and Elemental analysis data are available in ESM (Section S4). Copies of FT-IR and NMR spectra of compounds **3**-**8** and of GA-dendrimer (**9**) (Figure S7.1-S7.21) are available in Section S7 of ESM.

Morphology, size, and Z-potential of GAD (9) particles

The morphology and size of GAD particles were firstly investigated by scanning electron microscopy (SEM). In addition, the hydrodynamic size (diameter) and Z-potential (mV) of GA-dendrimer (**9**) particles were also determined by dynamic light scattering (DLS) analysis for further confirmation of SEM results.

Scanning electron microscopy The sample was fixed on aluminium pin stubs and sputter-coated with a gold layer (30 mA for 1 min) and was examined at an accelerating voltage of 20 kV. The micrographs were recorded digitally using DISS 5 digital image acquisition system (Point Electronic GmbH, Halle, Germany) and the average size of particles was provided by the instrument.

Scheme 1 Synthetic procedure for preparing GA-dendrimer **9**

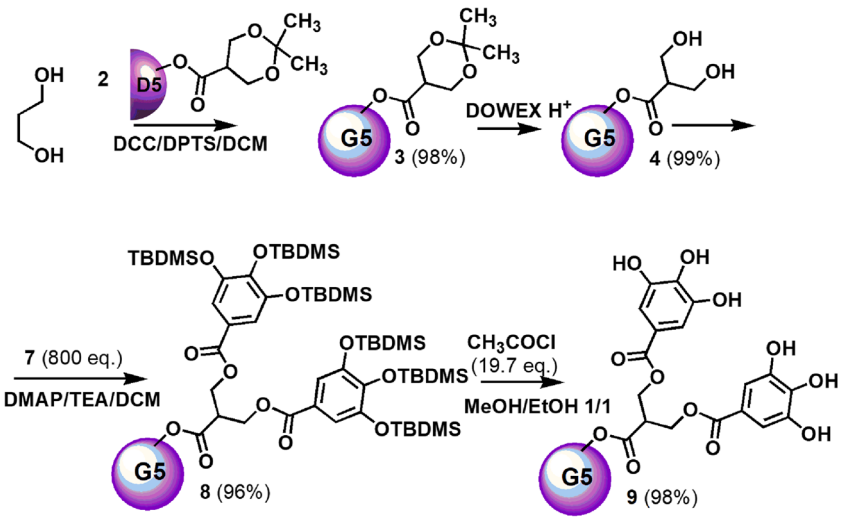

Dynamic light scattering The hydrodynamic size (diameter) of GAD was measured in batch mode at the physiological temperature of 37 °C in a low volume quartz cuvette (path length 10 mm) using a back scattering detector (173°, 633-nm laser wavelength). The dendrimer sample was prepared at a concentration of 1.0 mg/mL in in PBS and filtered through a 0.02-μm filter. A minimum of 12 measurements were performed. Z average diameter (Z-AVE), derived from a cumulants analysis of the measured correlation curve, was reported as the intensity-weighted average (Int-Peak) hydrodynamic radius. The Z-potential was measured at 37 °C in PBS as medium and an applied voltage of 100 V was used. The GAD sample was loaded into pre-rinsed folded capillary cells and twelve measurements were performed.

GAD antioxidant activity *in vitro* investigation

In order to evaluate the antioxidant power of GA-dendrimer (**9**), its radical scavenging activity (RSA %) has been determined by performing the DPPH• (2, 2-diphenyl-1-pycrylhydrazyl) assay. For comparison, commercially available samples of GA, ascorbic acid (AA) and Trolox, indicated as standards, were similarly essayed.

Determination of 1, 1-diphenyl-2-picryl hydrazyl radical scavenging activity of GA-dendrimer (9), GA, AA, and Trolox

The DPPH• (2, 2-diphenyl-1-pycrylhydrazyl) assay [56] was performed, to determine the radical scavenging activity (RSA) of GA-dendrimer (**9**), GA, AA, and Trolox. Briefly, aliquots (0.250 mL) of the water solutions of compounds under study were transferred into a 10-mL volumetric flask and a daily prepared DPPH mother solution (approximately 10^{-4} M in methanol) was added. Depending on the compounds solubility, the samples solutions were prepared in the range of concentration of 340–6760 μg/mL (GAD), 35–6760 μg/mL (AA), 25–6760 μg/mL (Trolox), and 17–6760 μg/mL (GA). The reaction flask was kept in the dark for 30 min, and the

Scheme 2 Synthetic three steps procedure for preparing acid chloride derivative of GA **7**, via compounds **5** and **6**

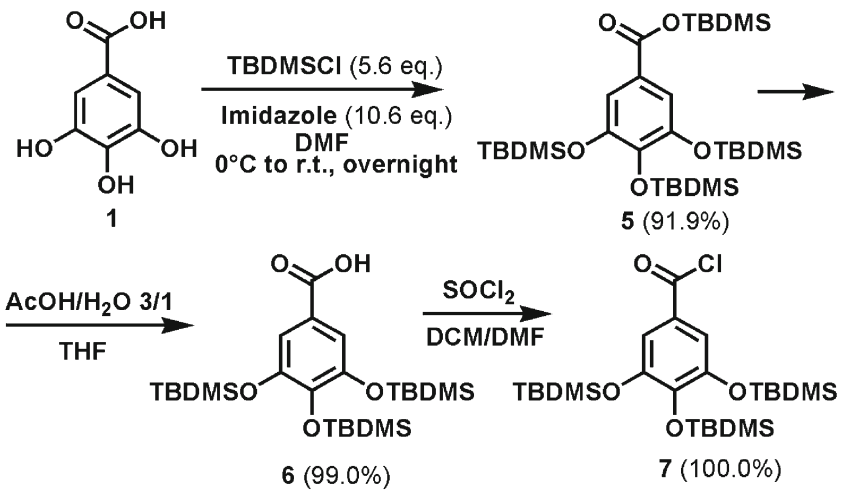

Table 1 Yield (%) of each reaction step performed, MW and physical state of compounds **3**-**9**

Entry (g; mmol)	Product (g; mmol; %)	Yield (%)	MW	Physical state
2	**3**	98.0	8557.28[a]	Glassy
2.64; 0.600	2.34; 0.27			Off-white solid
3	**4**	99.0	7275.24[a]	Fluffy white hygroscopic solid
2.34; 0.270	1.94; 0.267			
1	**5**	91.9[b]	626.37	Viscous resin
398.7; 2.34	1.35[b]; 2.15[b]			
5	**6**	99.0	512.90	White crystals
1.20; 1.91	0.94; 1.89			
6	**7**	100.0	531.35	Pale yellow waxy solid
0.93; 1.81	0.96; 1.81			
4	**8**	95.5[c]	Not isolated	Not isolated
159.3; 0.022	0.82[c]; 0.02[c]			
8	**9**	97.6	17,010.02[a]	Brownish glassy hygroscopic solid
1.00; 0.0256	0.43; 0.025			

[a] Estimated by ^{1}H NMR spectra and confirmed by Elemental analysis

[b] Weight, mmol, and yield have been calculated considering the impurities

[c] Not purified product

residual absorbance (A) was measured by an Agilent 8453 UV-VIS spectrophotometer at 515 nm, at 25 °C. For each sample, A was measured at different sample concentrations within the ranges reported above. Blanks (solution without samples) were measured before each sample and subtracted. The results were expressed as a percentage (%) of the DPPH free radical scavenging activity, calculated with the following Eq. (1):

$$Scavenging\ activity(\%) = \frac{[A(blank) - A(sample\ or\ standard) \times 100]}{A(blank)} \quad (1)$$

where *A* (blank) is the absorbance of DPPH radicals without sample or standard and *A* (sample or standard) is the absorbance of DPPH radicals with sample or standard, i.e. commercially available compounds. All the analytical determinations were developed in three replicated, and standard deviation (± SD) was calculated in order to assess the repeatability of the method.

Evaluation of biodegradability of GAD by performing an *in vitro* simulation of hydrolysis by cell esterase

Procedure for enzymatic hydrolysis of GA-dendrimer (9) by pig liver esterase

GA-dendrimer **9** (0.100 g, 0.0058 mmol) was dissolved in acetone (10 mL), then PBS phosphate buffer (pH = 7.4, 20 mL) was added. The solution was treated with pig liver esterase (PLE EC 3.1.1.1) lyophilised powder, ≥ 15 units/mg solid (50 mg). The mixture was stirred at physiological temperature (37 °C) for 24 h. The suspension was then filtered, through Celite plug, and the filtrate was extracted with ethyl acetate. The organic layer was dried over $MgSO_4$, filtered, and evaporated, to leave a crude product named **10**, as a brownish residue (0.0878 g). Firstly, **10** was qualitatively investigated (Section S6 in ESM), in order to define its composition and to identify its components. After having established by qualitative analysis on crude **10** that the main detectable component was GA (Section S6 in ESM), a recrystallisation from ethanol was performed, obtaining white crystals, to which the name **10c** was assigned (0.0632 g, 0.3715 mmol). **10c** was analysed by NMR spectroscopy and elemental analysis, that confirmed the structure of GA and a very good level of purity. Detailed characterisation data and copies of ^{1}H and ^{13}C NMR of **10c** are available in ESM (Section S6).

Enzymatic hydrolysis kinetic quantification by gas chromatography-mass spectrometry

Procedure A sample of GA-dendrimer (**9**) was subjected to enzymatic hydrolysis by performing the same procedure described above, taking aliquots of hydrolysate (1 mL) at different time points.

Each aliquot was extracted with ethyl acetate and rapidly dried over $MgSO_4$. The solvent was separated and removed and the residue was incubated with 250 μL of 1:1 *N, O*-bis(trimethylsilyl)trifluoroacetamide (BTSFA)/anhydrous pyridine at 70 °C.

Instrumental conditions Helium flow 39 ml/min; injector temperature 260 °C; transfer line temperature 280 °C; energy of electron 70 eV; oven temperature 90 °C for 1 min, from 90 to 240 °C at ramp rate of 20 °C/min, 240 °C for 10 min, from 240 to 280 °C at ramp rate of 20 °C/min, 280 °C for 1 min; split less injection mode was used to introduce 1 μL of sample. All experiments were done in duplicate repeating the analysis if the error between duplicate samples was greater than 5%.

In vitro GAD cytotoxicity evaluation by cell viability (%) determination

Cell culture

Epithelial (fibrosarcoma) B14 cells (Cricetulus griseus, ATCC, CCL-14.1, Sigma-Aldrich Inc.) were grown in high-glucose Dulbecco's modified Eagle medium with 10 % (*v*/*v*) fetal bovine serum (FBS) and 4 mM glutamine; liver BRL 3A cells (Rattus norvegicus, ATCC, CRL-1442, Sigma-Aldrich Inc.) with fibroblast-like morphology, were grown in Ham's F12 medium with 10% (*v*/*v*) FBS and 2 mM glutamine. All media were supplemented with 0.1% (*w*/*v*) penicillin and 0.1% (*w*/*v*) streptomycin. The cells were maintained in culture flasks in a 37 °C humidified atmosphere of 5% CO_2/95 % air (incubator) and passaged every 2–3 days. Cells were harvested and used in experiments after obtaining 80–90% confluence. The number of viable cells was determined by trypan blue exclusion with a haemo-cytometer. Then cells were suspended in media at a concentration of 1.0×10^{-5} cells per mL and plated in flat-bottom 96-well plates. Plates with cells were incubated for 24 h at 37 °C in a humidified atmosphere of 5% CO_2 to allow adherence of the cells before the administration of dendrimer.

3-(4, 5-Dimethylthiazol-2-yl)-2,5-diphenyltetrazolium bromide (MTT) assay

Cytotoxicity of GAD **9** was assayed with MTT. After 24-h incubation when cells attached on 96-well plates, they were treated with GAD at a concentration from 0.5 to 20 μmol/L (dimethylsulphoxide, DMSO). After 24-h incubation, a 20-μL solution of MTT in phosphate-buffered saline (5 mg/mL) was added to each well. Four hours later the medium was removed and the formazan precipitate was dissolved in DMSO for absorbance measurement at 580 nm and reference at 700 nm. The cell viability was related to the control wells, containing untreated cells with fresh cell culture medium and was calculated according to the following Eq. (2):

$$Cell\ viability(\%) = \frac{Absorption\ test}{Absorption\ control} \times 100 \qquad (2)$$

The results were presented as the mean of three measurements (± SD).

Statistical analyses

Data are expressed as means ± SD. Statistical significance of differences was determined by one-way analysis of variances (ANOVA). $P < 0.05$ was considered statistically significant.

Results and discussion

General considerations

As far as the planning of **4** is concerned, the choice of a high MW polyester-based dendrimer architecture and of the specific fifth generation has been pivoted on several considerations, dictated by the first aim of the present work, i.e. to improve GA stability, LHB, and gastrointestinal absorbability, to slow down its fast metabolism and to decrease its pro-oxidant counterpart.

Dendrimer architecture can both enhance oral drugs absorption and increase their blood residence time through three modality.

(i). Acting as "excipients" or permeability enhancers, dendrimers alter the barrier function of the intestinal epithelium and thereby enhance the permeability of a co-administered drug [52].
(ii). The dendrimer–drug complex may itself be better transported across the intestinal epithelium.
(iii). Big constructs with large surface and high molecular weight are typically retained in the circulation for longer periods and provide enhanced opportunity for acting to drugs [52].

The polyester-based scaffold, differently from well-working, but not biodegradable strongly cationic commercial PAMAMs, is designed to hydrolyse under physiological conditions thus resulting not toxic to cells [32, 50, 51].

Preliminary calculations were made, to determine the lipophilic hydrophilic balance (LHB) [57] of the GA-dendrimers obtainable in function of the generation of dendrimer carrier adopted. The fifth-generation architecture of **4** would have allowed achieving a GA-enriched dendrimer with a little lower LHB value than GA and with a slightly more hydrophobic character thus favouring its absorbability in GIT. On the contrary, the not too much low LHB value would permit GAD water solubility.

The several peripheral OH functions of **4** could be exploited for further esterification reactions and to bind a considerable number of bioactive GA units. In addition, by the esterification of **4** with GA, two goals would be rationally achieved at once.

The synthesis of a biodegradable dendrimer in possession of intrinsic antioxidant activity thanks to the numerous

peripheral units of GA and the 192 phenol groups, potentialities as semi-natural alternative device to treat diseases caused by the OS.

The preparation of a GA's prodrug, i.e. a GA's reservoir in possession of the nonpareil characteristics of dendrimers known as excellent materials for drug delivery and biomedical applications [21–29].

GA-enriched dendrimer **9** could have allowed the simultaneous transport of many GA moieties towards cells and, once inside the cells, thanks to its polyester-based structure, it would been degraded by the hydrolytic action of the cellular esterase, releasing GA for further antioxidant action.

Preparation of GA-enriched dendrimer (9)

On the base of the common practice of making use of nanoparticles to ameliorate solubility, GIT absorbability and metabolism profile of chemical bioactive entities with pharmacokinetics drawbacks, the fifth-generation polyester-based dendrimer **4** was prepared, and then, it was peripherally decorated with sixty-four GA units achieving the GA-enriched dendrimer **9** (Scheme 1).

Dendrimer **4** was synthetised by esterification of the diol *core*, i.e. 1, 3-propandiol, with the fifth generation dendron **2** (Fig. 2), owing a free carboxyl group, to achieve acetonide protected dendrimer **3**.

Subsequently, intermediate dendrimer **3** was exposed to acidic condition by treatment with Dowex resins to give **4** (Scheme 1). Table S1 (Section S1 in ESM) reports essential experimental data of all reaction performed in the present work. Table 1 summarises the percentage yield of each reaction step performed, together with the MW and physical state of compounds **3**-**9**.

Dendron **2** was in turn prepared via convergent, double exponential, and divergent growth approaches, using the AB2 type monomer 2, 2'-*bis*(hydroxymethyl)propionic acid (*bis*-HMPA) as building block [58]. Firstly, the fourth-generation dendron homologous of **2** both benzyl and acetonide protected to the carboxylic group and to the periphery respectively and named D4BnA (Fig. S1 in ESM) was prepared [53]. Then, its sixteen peripheral hydroxyls were set free by acidic treatment, to obtain the compound named D4BnOH (Fig. S1 in ESM). D4BnOH was increased by one generation, obtaining the fifth-generation dendron D5BnA (Fig. S1 in ESM), that, after catalytic hydrogenation to set free the carboxylic group, provided **2** as off-white foamy solid [54].

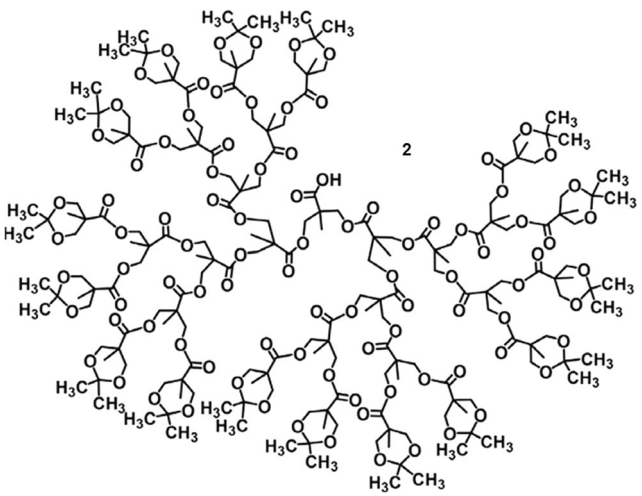

Fig. 2 Structure of the fifth generation dendron **2**

Both **3** and **4** were obtained in high yield and were characterised by FT-IR, NMR, and elemental analysis, which confirmed both the structure and the good level of purity.

Since GA **1** is a poly-functional substance and represents an AB2 type monomer itself, before esterification of **4**, some precautions have been taken, in order to avoid undesired and uncontrolled GA polymerisation.

Firstly, GA **1** was protected both to the three hydroxyls and the carboxyl group, with *tert*-butyldimethylsilyl chloride (TBDMSCl) obtaining **5** [59]. The derivative **5** was then transformed in **6** by selective removal of the TBDMS protecting group from carboxyl [59] and finally **6** was transformed in the chloride acid derivative **7** (Scheme 2).

An attempt to obtain the derivative **6** in a single step [60] provided a mixture of **6** and **5** that would have required chromatographic separation, so that the above described, longest but most convenient procedure, was preferred.

The conversion of **6** in **7** was realised implementing the common procedure that uses $SOCl_2$ with small amounts of DMF as catalyst. Thanks to the *in situ* formation of a reactive chloroiminium intermediate (Vilsmeier–Haack reagent), which is ideal as a halogenating reagent [61–64], the complete substitution of OH with chlorine atom was achieved in less than 2 h. The structure of all the compounds was confirmed by FT-IR, NMR, and elemental analysis. NMR spectra of **5** showed the presence of two impurities, not previously highlighted [59]. These pollutants, identified as 1, 3-di-*tert*-butyl-1, 1, 3, 3-tetramethyl-disiloxane, (5.6%) and 1, 2-di-*tert*-butyl-1, 1, 2, 2-tetramethyldisilane (6.0%) were easily removed in the next step during crystallisation of compound **6**. Elemental analysis was not influenced by the presence in traces of these impurities. The last two reaction steps (Scheme 1) allowed achieving the GA-decorated dendrimer **9**. The intermediate TBDMS-GA-dendrimer **8** was analysed by FT-IR (Fig. S7.18 in ESM), and all the spectrum signals were consistent with the desired structure and gave proof of the successful coupling between **4** and **7**. Then, since an investigation by TLC of crude **8** showed only trivial traces of unreacted **7**, it was subjected to TBDMS removal reaction, without further purification, postponing it to the next final step. As reaction system, acidic conditions by anhydrous hydrochloric acid generated *in situ* from acetyl chloride and alcohols was selected. The reported procedure [65], that avoids

water, would be respectful of the polyester architecture of **8** and, even if slightly modified, has been already extensively exploited by the authors in previous works [58, 66, 67] to remove BOC protecting group from similarly structured polyester-based dendrimers. Differently from the reported procedure [65], the reaction was developed using a strong excess of acetyl chloride [58, 66, 67]. The complete deprotection was achieved within 5 h at r.t. After purifying procedures developed to remove the residual unbound GA, GA-dendrimer (**9**) was obtained as brownish glassy hygroscopic solid that, in the $FeCl_3$ test for the identification of phenols, gave a green colouring (Fig. S3.1 in ESM). Otherwise, from free GA, that in such test gives dark blue or black colouring (Fig. S6.1, ESM), green colouring is characteristic of high molecular weight GA esters as Gallotannins [68], thus indicating the absence of unassociated GA and the good outcome of purification procedure. Structure of GA-dendrimer (**9**) was further confirmed by FT-IR, Elemental analysis and NMR. In particular, as a consequence of esterification, changes in the ^{1}H NMR spectrum of **4** were observed around 4.00 ppm, but the GA presence was definitively asserted by a very intense peak concerning the CH = proton atoms of the GA aromatic ring at 7.30 ppm.

Morphology, size, and Z-potential of GAD particles

SEM images of the GA-enriched dendrimer (**9**) are shown in Fig. 3 while in Table 2, the average particles size provided by the instrument has been reported.

As all we know, particles size of about 380 nm is uncommon for dendrimers of similar generation [69], but is typical for the so called megamers [70]. Megamers are dendrimer multi-molecular assemblies that, besides occurring thanks to cross-linking agents introduced during the synthesis, can form also because of the natural clustering assemblies of dendrimer molecules into supramolecular assemblies. In the present case, such an assembly process was rationally favoured by the several poly hydroxylated GA units that can establish many hydrogen bonds between the dendrimer molecules, giving rise to dendrimers aggregates. Dendrimer particles, in SEM image, appear amazingly spherical and consequently gifted with a very large surface area that typically increases the DDSs systemic retention time and their bio-efficiency [52]. For further confirmation of SEM results, the particle hydrodynamic size (diameter) of GAD was measured using DLS analysis and the result matched the SEM ones with a very small error of 12 nm. It was reported as the intensity-weighted average (Z-AVE) [*N* (degree of freedom) = 12] in Table 2. In addition, by DLS technique, Z-potential (mV) of GA-dendrimer (**9**) particles was also measured, for having an idea of physical stability of GAD in aqueous solution, for investigating the possible tendency of the GAD particles to form aggregates (megamers) and therefore obtaining a further validation of the assumption referred to above, and for inquiring possible toxicity. The result was reported in Table 2.

Zeta potential is the potential difference between the dispersion medium and the stationary layer of fluid attached to particles. It is a measure of the electrical charge of particles that are suspended in liquid and is crucial also for nanoparticles-cell interactions. Low Z-potential favours the particles binding to low serum proteins and a longer

Table 2 GAD particle hydrodynamic size (DLS) and Z-potential at 37 °C (± SD), average particles size by SEM analysis and cell viability values (± SD) from cytotoxicity essay at GAD concentration of 340 μg/mL

Z-AVE size (nm)[a]	Average particles size (nm) by SEM analysis	Z-potential (mV)[a]	Cell viability (%)[b]	
375 ± 7.9	387 ± 11	− 25 ± 0.34	B14	BRL
			91.4 ± 3.5	85.3 ± 1.1

[a] N (degree of freedom) = 12

[b] N (degree of freedom) = 3

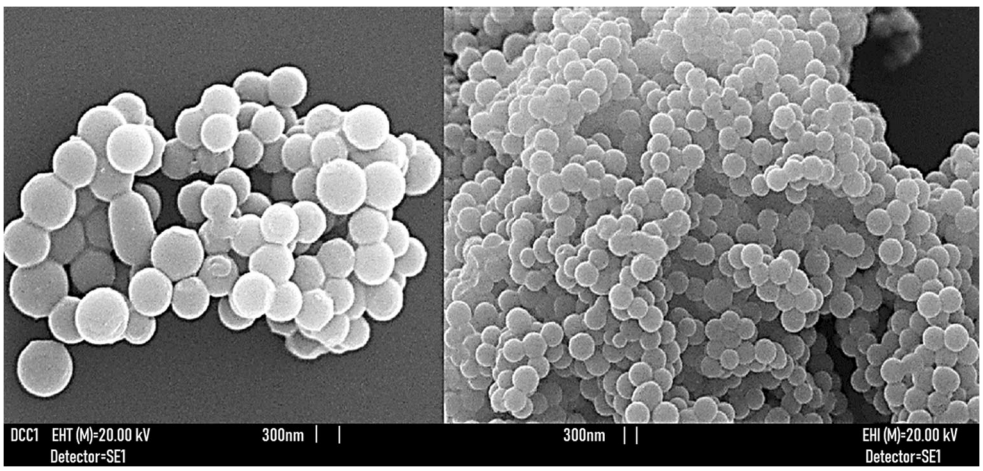

Fig. 3 SEM images of GA-enriched dendrimer particles

circulation in blood. Values < 5 mV may lead to agglomeration of particles conferring physical instability in solution. On the contrary, Z-potential > 30 mV, either positive or negative, leads to monodispersity and good physical stability in solution [71, 72]. Finally, high positive Z-potential values are correlated to high cytotoxicity while negative values allow high cell viability [73]. In these regards, the GA-dendrimer (**9**) nanoparticles here prepared, possess a Z-potential of − 25 mV ± SD and therefore can be considered sufficiently stable in water solution, with a tendency to form megamer aggregates as supposed by the average particles size by SEM and DLS, and would be endowed with low cytotoxicity.

Radical scavenging activity of GA-dendrimer (9)

In order to evaluate the antioxidant power of GA-dendrimer (**9**) the radical scavenging activity (RSA %) was determined by the DPPH• assay [56]. In parallel, for comparison purposes, samples of commercially available GA, AA, and Trolox have been tested in the same conditions. The RSA (%) was evaluated at different concentrations of GA-dendrimer (**9**), GA, AA, and Trolox and reported in graphs as functions of concentrations. Concentrations were expressed in μg/mL, μmol/mL, and in molarity (mM) (Fig. S5.1 in ESM). The results were then expressed as IC_{50} that is the efficient concentration of sample that inhibits 50% of the DPPH radicals [74].

Table S1. in ESM shows the determined IC_{50} expressed in μg/mL, μmoL/mL, and millimolarity again, together with an IC_{50} value of α-tocopherol (Vitamin E) reported in literature.

Since the molecular weight of GAD is considerably higher than that of GA, AA, Trolox, and α-tocopherol, it is more consistent to compare molar concentrations rather than the concentrations in weight. According to these results, as early supposed, GA-dendrimer (**9**) proved to possess an intrinsic antioxidant activity even higher than that of Trolox, AA, GA, and vitamin E. GAD proved to reach the IC_{50} action at molar concentrations of 24, 15, 4, and 3 times more diluted respectively (Fig. 4).

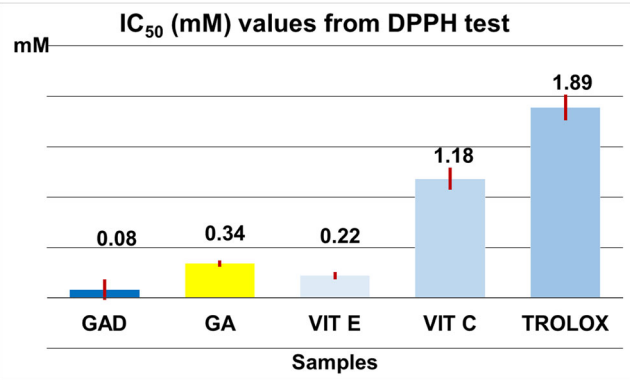

Fig. 4 Comparison between radical scavenging activity expressed as IC_{50} (mM) of **9**, GA, Vitamins A and E and Trolox

In order to investigate the effect of heat on the antioxidant property of GA-dendrimer (**9**) and GA, samples of GAD and GA were dissolved in ethanol at the highest possible concentration (6.67 mg/mL), heated until the solution was browned and evaluated for RSA % again.

In the case of GAD, RSA (%) turned out to be decreased of almost 60% if compared with RSA (%) determined on a not heated sample of **9** at same concentration (6.67 mg/mL), whereas in the case of GA, RSA (%) resulted decreased up to 98%. According to these results, GAD can be considered far more stable than GA to thermal induced oxidative degradation.

In vitro simulation of physiological cell esterase hydrolytic action

As it is extensively reported concerning polyester-based dendrimers [32, 50, 51], once inside the cell, GA-dendrimer (**9**) that belong to that category, it is supposed to undergo an enzymatic attack by cell esterase, that should degrade it, to small monomeric units, releasing GA. In order to have an experimental confirmation of this assumption, as last experience of this study, an *in vitro* reproduction of these events, was conceived and realised. Supposing an administration via i. v. and a high accumulation of GAD in liver, as reported by Palidda et al. [50] for high MW polyester-based analogous dendrimers, PLE was selected as model esterase. GAD was treated at physiological temperature and pH with the powdery form of PLE, which belongs to mammalian liver microsomal carboxylesterases. The solid residue obtained, named **10**, was then qualitatively investigated to evaluate its composition and its components identity. Firstly, investigations by $FeCl_3$ essay and TLC analysis were performed. The $FeCl_3$ essay on a crude **10** ethanol solution gave a blue colouring, identical to that given by a GA solution (Section S6, Fig. S6.1 in ESM), while TLC elution profile, showed as unique significant spot, a stain with the same Rf. of GA (Section S6, Fig. S6.2 in ESM). According to these qualitative investigation, GA was the main component of crude **10**. To complete the investigation, a recrystallisation of crude **10** was tried in the condition reported in literature for GA (hot ethanol). Off-white crystals (**10c**) were obtained whose m. p., NMR and elemental analysis confirmed the GA structure (Section S6 and Fig. S6.3 in ESM). The weight of **10c** and the mole number derived (64.05 mmol) were in accordance with the number (64) of the estimated (^{1}H NMR) GA units peripherally present per dendrimer mole with an error of less than + 0.08 %. Once identified that the main product UV-detectable of hydrolysis product was GA **1**, the enzymatic hydrolysis was repeated, to investigate the hydrolysis profile and to quantify the esterase hydrolysis kinetic. Another sample of GA-dendrimer (**9**) was treated with PLE again, and the GA content in hydrolysate was determined at different time points by GC/MS, after derivatisation of GA by

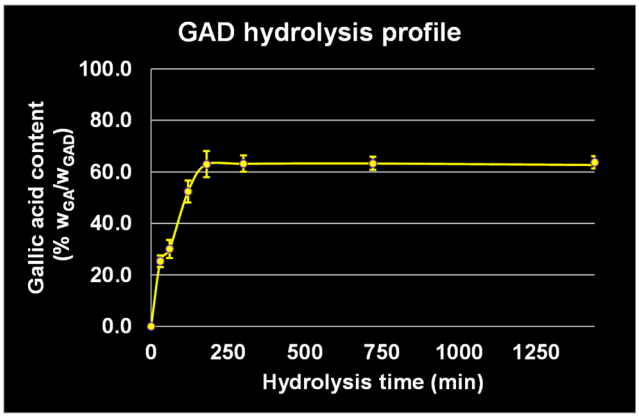

Fig. 5 Esterase hydrolysis profile [w_{GA}, weight of GA; w_{GAD}, weight of GA-dendrimer (**9**) treated with PLE (100 mg)]

using BTSFA. Figure 5 shows the results that highlighted a plateau of hydrolysis and therefore the GA maximum concentration within three hours.

In vitro cytotoxicity investigation by cell viability (%) evaluation

To determine the actual biomedical applications of GAD, its *in vitro* cytotoxicity profile, was investigated against two model cell lines, i.e. epithelial B14 and liver BRL cells. These particular cell lines where selected because they are particularly sensitive to tannic, ellagic, and gallic acids [75]; therefore, a good cell viability would have been meant, both as the low cytotoxicity of GAD and as the positive action of dendrimer architecture in reducing toxicity of GA versus these specific cell lines. MTT assay, a method which is based on monitoring of NAD(P)H-dependent cellular oxidoreductase enzyme activity and is therefore related to inhibition of metabolic processes in mitochondria, was performed. GAD concentration used in MTT assay was in the range 0.5–20 μmol/L according to literature data [76]. Regarding GAD, this range means a concentration of 8.5–340 μg/mL. The results referring to the fixed max concentration essayed only marginally affected cell growth, since viability values were in the range of > 90 % for B14 cells and > 82 % for BRL cells (Table 2).

Conclusions

The present work reports innovative and outstanding results that meet the needs of one of the most important research areas. Such current studies aims at optimising the antioxidant properties of natural polyphenols and at improving their drawbacks through the use nanosized carriers, for preparing innovative DDSs with potentialities as alternative more efficient therapeutics with reduced side effects.

By merging the nonpareil properties of synthetic dendrimers and the irreproducible multi-target health activity of natural compounds, a GA-enriched biodegradable and non-cytotoxic dendrimer (**9**), endowed with remarkable antioxidant power and nanoparticles amazingly spherical of about 380 nm, due to hydrogen bond induced aggregation to supramolecular megamers, was achieved. Aggregation of GAD nanoparticles is rationally favoured by Z-potential value (−25 mV) which, however, allows a sufficient stability in aqueous solution. GAD nanoparticles are gifted with very large surface area that typically increases the systemic retention time of DDSs and their bio-efficiency. GAD cytotoxicity investigations on two cell lines proved high viability (%) of cells exposed to GAD, its high degree of biocompatibility and an advantageous action of the carrier dendrimer scaffold in reducing the proven cytotoxicity of GA *versus* the cells tested. Thanks to these features, GA-dendrimer (**9**) is advisable for further more in deep investigations to evaluate its specific pharmacological activities and its eligibility as innovative therapeutic, against diseases triggered by OS. In this regard, as crucial property, GA-dendrimer (**9**) radical scavenging activity was investigated. GAD proved to be an antioxidant more powerful than free GA than other known antioxidants. Furthermore, as a GA delivering system, it is able to carry sixty-four GA units per mole at once, and when subjected to the attack by PLE, selected as an esterase model in physiological condition, it degrades, setting free the GA moieties transported, for further antioxidant activity. It can also be rationally thought that the GAD strong antioxidant activity may be exploited to reduce the auto-oxidative degradation of fatty acids, lipids, and foods or to prepare nanocomposites for the creation of active food packaging with a large positive economic impact.

Acknowledgements The authors are very thankful to Mr. Gagliardo Osvaldo for Elemental Analysis and Prof. Deirdre Kantz for language help.

As the first author, I affectionately dedicate this work to my dear parents and dear friend Rocco.

Funding information This work has been supported by University of Genoa (Progetti di Ateneo).

Compliance with ethical standards

Conflict of interest The authors declare that they have no conflict of interest.

References

1. Badhani B, Sharma N, Kakkar R. Gallic acid: a versatile antioxidant with promising therapeutic and industrial applications. RSC Adv. 2015;5:27540–57.

2. de la Rosa LA, Alvarez-Parrilla E, Gonzalez-Aguilar GA. Fruit and vegetable phytochemicals: chemistry, nutritional value and stability. Wiley-Blackwell Hoboken: New Jersey; 2016.
3. Booth AN, Masri MS, Robbins DJ, Emerson OH, Jones FT, Deeds F. The metabolic fate of gallic acid and related compounds. J Biol Chem. 1959;234:3014–6.
4. Madsen HL, Bertelsen G. Spices as antioxidants. Trends Food Sci Technol. 1995;6:271–7.
5. Nakatani N. Natural antioxidants from spices. In: Huang MT, Ho CT, Lee CY, editors. Phenolic compounds in food and their effects on health II. Antioxidants and cancer prevention. Washington, DC: ACS American Chemical Society; 1992. p. 72–86.
6. Cholbi MR, Paya M, Alcaraz MJ. Inhibitory effects of phenolic compounds on CCl4-induced microsomal lipid peroxidation. Experientia. 1991;47:195–9.
7. Filipiak K, Hidalgo M, Silvan JM, Fabre B, Carbajo RJ, Pineda-Lucena A, et al. Dietary gallic acid and anthocyanin cytotoxicity on human fibrosarcoma HT1080 cells. A study on the mode of action. Food Funct. 2014;5:381–9.
8. Sakagami H, Satoh K. Prooxidant action of two antioxidants: ascorbic acid and gallic acid. Anticancer Res. 1997;17:221–4.
9. Inoue M, Suzuki R, Sakaguchi N, Li Z, Takeda T, Ogihara Y, et al. Selective induction of cell death in cancer cells by gallic acid. Biol Pharm Bull. 1995;18:1526–30.
10. Bhattacharyya S, Ahammed SM, Saha BP, Mukherjee PK. The gallic acid phospholipid complex improved the anti oxidant potential of gallic acid by enhancing its bioavailability. AAPS Pharm Sci Technol. 2013;14:1025–33.
11. Ferruzzi MG, Lobo JK, Janle EM, Whittaker N, Cooper B, Simon JE, et al. Bioavailability of gallic acid and catechins from grape seed polyphenol extract is improved by repeated dosing in rats: implications for treatment in Alzheimer's Disease. Alzheimer Dis. 2009;18:113–24.
12. Konishi Y, Hitomi Y, Yoshioka E. Intestinal absorption of p-coumaric and gallic acids in rats after oral administration. J Agric Food Chem. 2004;52:2527–32.
13. Yasuda T, Inaba A, Ohmori M, Endo T, Kubo S, Ohsawa K. Urinary metabolites of gallic acid in rats and their radical-scavenging effects on 1,1-diphenyl-2-picrylhydrazyl radical. J Nat Prod. 2000;63:1444–6.
14. Alves ACS, Mainardes RM, Khalil NM. Nanoencapsulation of gallic acid and evaluation of its cytotoxicity andantioxidant activity. Mater Sci Eng. 2016;60:126–34.
15. Da Rocha LG, Bonfanti Santos D, Colle D, Gasnhar Moreira EL, Daniel Prediger R, Farina M, et al. Improved neuroprotective effects of resveratrol-loaded polysorbate 80-coated poly(lactide) nanoparticles in MPTP-induced Parkinsonism. Nanomedicine (London). 2015;10:1127–38.
16. Nahak P, Karmakar G, Chettri P, Roy B, Guha P, Besra SE, et al. Influence of lipid core material on physicochemical characteristics of an ursolic acid-loaded nanostructured lipid carrier: an attempt to enhance anticancer activity. Langmuir. 2016;32:9816–25.
17. Hu X, Liu G, Li Y, Wang X, Liu S. Cell-penetrating hyperbranched polyprodrug amphiphiles for synergistic reductive milieu-triggered drug release and enhanced magnetic resonance signals. J Am Chem Soc. 2015;137:362–8.
18. Li X, Qian Y, Liu T, Hu X, Zhang G, You Y, et al. Amphiphilic multiarm star block copolymer-based multifunctional unimolecular micelles for cancer targeted drug delivery and MR imaging. Biomaterials. 2011;32:6595–605.
19. Gao Y, Li Z, Xie X, Wang C, You J, Mo F, et al. Dendrimeric anticancer prodrugs for targeted delivery of ursolic acid to folate receptor-expressing cancer cells: synthesis and biological evaluation. Eur J Pharm Sci. 2015;70:55–63.
20. Madaan K, Kumar S, Poonia N, Lather V, Pandita D. Dendrimers in drug delivery and targeting: drug-dendrimer interactions and toxicity issues. J Pharm Bioallied Sci. 2014;6:139–50.
21. Xu J, Luo S, Shi W, Liu S. Two-stage collapse of unimolecular micelles with double thermoresponsive coronas. Langmuir. 2006;22:989–97.
22. Luo S, Xu J, Zhu Z, Wu C, Liu S. Phase transition behavior of unimolecular micelles with thermoresponsive poly(N-isopropylacrylamide) coronas. J Phys Chem. 2006;110:9132–9.
23. Xu H, Xu J, Jiang X, Zhu Z, Rao J, Yin J, et al. Thermosensitive unimolecular micelles surface-decorated with gold nanoparticles of tunable spatial distribution. Chem Mater. 2007;19:2489–95.
24. Luo S, Hu X, Ling C, Liu X, Chen S, Han M. Multiarm star-like unimolecular micelles with a dendritic core and a dual thermosensitive shell. Polym Int. 2011;60:717–24.
25. Kesharwani P, Jain K, Jain NK. Dendrimer as nanocarrier for drug delivery. Prog Polym Sci. 2014;39:268–307.
26. Satija J, Sai VVR, Mukherji S. Dendrimers in biosensors: concept and applications. J Mater Chem. 2011;21:14367–86.
27. Caminade AM. Dendrimers as biological sersors. In: Caminade AM, Turrin CO, Laurent R, Ouali A, Delavaux-Nicot B, editors. Dendrimers: towards catalytic, material and biomedical uses. Chichester: John Wiley and Sons Ltd Inc.; 2011. p. 375–92.
28. Kim J-H, Park K, Nam HY, Lee S, Kim K, Kwon IC. Polymers for bioimaging. Prog Polym Sci. 2007;32:1031–53.
29. Wang Z, Niu G, Chen X. Polymeric materials for theranostic applications. Pharm Res. 2014;31:1358–76.
30. Lee CC, MacKay JA, Frechet JMJ, Szoka FC. Designing dendrimers for biological applications. Nat Biotechnol. 2005;23:1517–26.
31. Hourani R, Kakkar A. Advances in the elegance of chemistry in designing dendrimers. Macromol Rapid Commun. 2010;31:947–74.
32. De Jesus OLP, Ihre HR, Gagne L, Frechet JMJ, Szoka FC. Polyester dendritic systems for drug delivery applications: in vitro and in vivo evaluation. Bioconjug Chem. 2002;13:453–61.
33. Alfei S, Taptue GB, Catena S, Bisio A. Synthesis of water-soluble, polyester-based dendrimer prodrugs for exploiting therapeutic properties of two triterpenoid acids. Chin J Polym Sci. 2018;36:999–1010.
34. Alfei S, Catena S, Ponassi M, Rosano C, Zoppi V, Spallarossa A. Hydrophilic and amphiphilic water-soluble dendrimer prodrugs suitable for parenteral administration of a non-soluble non-nucleoside HIV-1 reverse transcriptase inhibitor thiocarbamate derivative. Eur J Pharm Sci. 2018;124:153–64.
35. Alfei S, Turrini F, Catena S, Zunin P, Parodi B, Zuccari G, et al. Pectin microdispersion vs non-polyamidoamine dendrimer nanodispersions: two biocompatible approaches to increase Ellagic Acid water solubility and allow its more ways therapeutic administration. New J Chem. 2019;43:2438–48.
36. Kaminskas LM, McLeod VM, Kelly BD, Cullinane C, Sberna G, Williamson M, et al. Association of chemotherapeutic drugs with dendrimer nanocarriers: an assessment of the merits of covalent conjugation compared to noncovalent encapsulation. Mol Pharm. 2012;9:422–32.
37. Oliveira JM, Salgadoc AJ, Sousa N, Mano JF, Reis RL. Dendrimers and derivatives as a potential therapeutic tool in regenerative medicine strategies—a review. Prog Polym Sci. 2010;35:1163–94.
38. Wang W, Chen L-J, Wang X-Q, Sun B, Li X, Zhang Y, et al. Organometallic rotaxane dendrimers with fourth-generation mechanically interlocked branche. PNAS. 2015;112:5597–601.
39. Mohammadifar E, Kharat AN, Adeli M. Polyamidoamine and polyglycerol; their linear, dendritic and linear–dendritic architectures as anticancer drug delivery systems. J Mater Chem B. 2015;3:3896–921.

40. Xu X, Li J, Han S, Tao C, Fang L, Sun Y, et al. A novel doxorubicin loaded folic acid conjugated PAMAM modified with borneol, a nature dual-functional product of reducing PAMAM toxicity and boosting BBB penetration. Eur J Pharm Sci. 2016;88:178–90.
41. Jain K, Kesharwani P, Gupta U, Jain NK. Dendrimer toxicity: let's meet the challenge. Int J Pharm. 2010;394:122–42.
42. Chang KL, Higuchi Y, Kawakami S, Yamashita F, Hashida M. Development of lysine-histidine dendron modified chitosan for improving transfection efficiency in HEK293 cells. J Control Release. 2011;156:195–202.
43. Wen Y, Guo Z, Du Z, Fang R, Wu H, Zeng X, et al. A review of nanocarriers for the delivery of small interfering RNA. Biomaterials. 2012;33:8111–21.
44. Wang F, Wang Y, Wang H, Shao N, Chen Y, Cheng Y. Synergistic effect of amino acids modified on dendrimer surface in gene delivery. Biomaterials. 2014;35:9187–98.
45. Liu X, Liu C, Zhou J, Chen C, Qu F, Rossi JJ, et al. Promoting siRNA delivery via enhanced cellular uptake using an arginine-decorated amphiphilic dendrimer. Nanoscale. 2015;7:3867–75.
46. Ihre HR, De Jesus POL, Szoka FC Jr, Frechet JMJ. Polyester dendritic systems for drug delivery applications: design, synthesis, and characterization. Bioconjug Chem. 2002;13:443–52.
47. Quadir MA, Haag R. Biofunctional nanosystems based on dendritic polymers. J Controlled Release. 2012;161:484–95.
48. Zhou Z, Tang J, Sun Q, Murdoch WJ, Shen Y. A multifunctional PEG–PLL drug conjugate forming redox-responsive nanoparticles for intracellular drug delivery. J Mater Chem B. 2015;3:7594–603.
49. Gillies ER, Fréchet JMJ. Dendrimers and dendritic polymers in drug delivery. Drug Discov Today. 2005;10:35–43.
50. Ma X, Zhou Z, Jin E, Sun Q, Zhang B, Tang J, et al. Facile synthesis of polyester dendrimers as drug delivery carriers. Macromolecules. 2013;46:37–42.
51. Ma X, Tang J, Shen Y, Fan M, Tang H, Radosz M. Facile synthesis of polyester dendrimers from sequential click coupling of asymmetrical monomers. J Am Chem Soc. 2009;131:14795–803.
52. Kaminskas LM, Boyd BJ, Porter CJH. Dendrimer pharmacokinetics: the effect of size, structure and surface characteristics on ADME properties. Nanomedicine (London). 2011;6:1063–84.
53. Ihre H, Hult A, Fréchet JMJ, Gitsov I. Double-stage convergent approach for the synthesis of functionalized dendritic aliphatic polyesters based on 2,2-bis(hydroxymethyl)propionic acid. Macromolecules. 1998;31:4061–8.
54. Alfei S, Castellaro S. Synthesis and characterization of polyester-based dendrimers containing peripheral arginine or mixed amino acids as potential vectors for gene and drug delivery. Macromol Res. 2017;25:1172–86.
55. Alfei S, Castellaro S, Taptue GB. Synthesis and NMR characterization of dendrimers based on 2, 2-bis-(hydroxymethyl)-propanoic acid (bis-HMPA) containing peripheral amino acid residues for gene transfection. Org Commun. 2017;10:144–77.
56. Brand-Williams W, Cuvelier ME, Berset C. Use of a free radical method to evaluate antioxidant activity. Food Sci Technol. 1995;28:25–30.
57. Griffin CC. Calculation of HLB values of non-ionic surfactants. J Soc Cosmet Chem. 1954;5:249–56.
58. Carlmark A, Malström E, Malkoch M. Dendritic architectures based on bis-MPA: functional polymeric scaffolds for application-driven research. Chem Soc Rev. 2013;42:5858–79.
59. Malik G, Natangelo A, Charris J, Pouységu L, Manfredini S, Cavagnat D, et al. Synthetic studies toward C-glucosidic ellagitannins: a biomimetic total synthesis of 5-O-desgalloylepipunicacortein A. Chem Eur J. 2012;18:9063–74.
60. Ma H, Wang L, Niesen DB, Cai A, Cho BP, Tan W, et al. Structure activity related, mechanistic, and modeling studies of gallotannins containing a glucitol-core and α-glucosidase. RSC Adv. 2015;5:107904–15.
61. Stadler PA. Eine einfache Veresterungsmethode im Eintopf-Verfahren. HCA. 1978;61:1675–81.
62. Marson CM. Reactions of carbonyl compounds with (monohalo) methyleniminium salts (vilsmeier reagents). Tetrahedron. 1992;48:3659–726.
63. Clayden J. Organolithiums: selectivity for synthesis. Oxford: Pergamon; 2002.
64. Ansell MF. Preparation of acyl halides. In: Patai S, editor. The chemistry of acyl halides. Bristol: John Wiley and Sons; 1972. p. 35–64.
65. Khan AT, Mondal EA. Highly efficient and useful synthetic protocol for the cleavage of tert-butyldimethylsilyl(TBS) ethers using a catalytic amount of acetyl chloride in dry methanol. Synlett. 2003;5:694–8.
66. Alfei S, Catena S. Synthesis and characterization of versatile amphiphilic dendrimers peripherally decorated with positive charged amino acids. Polym Int. 2018;67:1572–84.
67. Alfei S, Catena S. Synthesis and characterization of fourth generation polyester-based dendrimers with cationic amino acids-modified crown as promising water soluble biomedical devices. Polym Adv Technol. 2018;29:2735–49.
68. Falcão L, Araújo MEM. Tannins characterisation in new and historic vegetable tanned leathers fibres by spot tests. J Cult Herit. 2011;12:149–56.
69. Chaudhari HS, Popat RR, Adhao VS, Shrikhande VN. Dendrimers: novel carrier for drug delivery. J App Pharm Res. 2016;4:1–19.
70. Manjappa K, Narayanaswamy J. Thiol−disulfide interchange mediated reversible dendritic megamer formation and dissociation. Macromolecules. 2009;42:7353–9.
71. Joseph E, Singhvi G. Multifunctional nanocrystals for cancer therapy: a potential nanocarrier. In: Grumezescu AM, editor. Nanomaterials for Drug Delivery and Therapy. Amsterdam: Elsevier; 2019. p. 91–111.
72. Lu GW, Gao P. Emulsions and microemulsions for topical and transdermal drug delivery. In: Kulkarni VS, editor. Handbook of non-invasive drug delivery systems. Amsterdam: Elsevier; 2010. p. 59–94.
73. Shao X-R, Wei X-Q, Song Z, Hao L-Y, Cai X-X, Zhang Z-R, et al. Independent effect of polymeric nanoparticle zeta potential/surface charge, on their cytotoxicity and affinity to cells. Cell Prolif. 2015;48:465–74.
74. Gawron-Gzella A, Dudek-Makuch M, Matławska I. DPPH radical scavenging activity and phenolic compound content in different leaf extracts from selected blackberry species. Acta Biol Cracov Ser Bot. 2012;54:32–8.
75. Labieniec M, Gabryelak T. Effects of tannins on Chinese hamster cell line B14. Mutat Res Genet Toxicol Environ Mutagen. 2003;539:127–35.
76. Dobrovolskaia MA, Patri AK, Simak J, Hall JB, Semberova J, De Paoli Lacerda SH, et al. Nanoparticle size and surface charge determine effects of PAMAM dendrimers on human platelets in vitro. Mol Pharm. 2012;9:382–93.